PREPRINT

PERTANIKA JOURNALS

SCIENCE & TECHNOLOGY

Journal homepage: http://www.pertanika.upm.edu.my/

Extraction and Characterisation of Natural Fibres from *Pennisetum purpureum*: Influence of Harvesting Age on Chemical, Mechanical, and Thermal Properties

Mohd Fairus Kayat[1], Ridhwan Jumaidin[1,2]*, Mastura Mohamad Taha[1] and Fahmi Asyadi Md Yusof[3]

[1]Fakulti Teknologi dan Kejuruteraan Industri dan Pembuatan, Universiti Teknikal Malaysia Melaka, Hang Tuah Jaya, 76100 Durian Tunggal, Melaka, Malaysia
[2]Mechanical Engineering Programme, Faculty of Engineering, Universiti Malaysia Sabah, Jalan UMS, 88400 Kota Kinabalu, Sabah, Malaysia
[3]Malaysian Institute of Chemical and Bioengineering Technology, Taboh Naning, 78000 Alor Gajah, Melaka, Malaysia

ABSTRACT

This study examined new bio-based, natural cellulosic fibres from the *Pennisetum purpureum* plant, determining the optimal harvesting age at 30, 45, and 60 days for the first time. The fibres were extracted using a water-retting process and investigated for their potential as reinforcement materials in polymer composites. The characterisation process involved analysing the fibre's chemical composition, as well as its physical, thermal, mechanical, crystallinity, and morphological properties. Chemical composition was determined using standard chemical analysis, while mechanical properties were evaluated through tensile testing. X-ray diffraction (XRD) was used to assess the fibre's crystallinity, and thermogravimetric analysis (TGA) measured thermal stability. Additionally, scanning electron microscopy (SEM) was employed to study the fibre's surface morphology. The results indicated that mechanical properties were influenced by the ratio of cellulose to lignin. At 30 days, the fibre achieved optimal mechanical performance due to an elevated lignin concentration counteracting reduced cellulose levels (tensile strength: 67.54 MPa, modulus: 3.14 GPa, cellulose: 35.61%, lignin: 16.47%). This highlights that optimal fibre performance depends on the interaction of chemical constituents rather than cellulose content alone. XRD analysis revealed that the crystallinity index of *P. purpureum* fibres was 51.19, 49.40, and 50.56% for 30-, 45-, and 60-day fibres, respectively, with the highest value at 30 days, suggesting better molecular organisation due to reduced amorphous components. Thermogravimetric

ARTICLE INFO

Article history:
Received: 24 February 2025
Accepted: 29 April 2025
Published: 25 September 2025

DOI: https://doi.org/10.47836/pjst.33.6.04

E-mail addresses:
mfairus.kayat@gmail.com (Mohd Fairus Kayat)
ridhwanj@ums.edu.my (Ridhwan Jumaidin)
mastura.taha@utem.edu.my (Mastura Mohamad Taha)
fahmiasyadi@unikl.edu.my (Fahmi Asyadi Md Yusof)
* Corresponding author

analysis showed that fibre age affected thermal degradation, with older fibres exhibiting greater hemicellulose breakdown and improved thermal stability. The 45-day fibre had the lowest moisture loss (4.78%) and the highest char residue (28.54%), indicating better thermal resistance than the 30- and 60-day fibres. The main weight loss due to cellulose and hemicellulose decomposition occurred between 276–390°C, with the 60-day fibre showing a slightly higher peak degradation temperature (390°C), suggesting a more structured cellulose composition. SEM analysis revealed that the fibre surface was perforated and coarse, with a central lumen, further supporting its potential as a reinforcing material in thermoplastic green composites. This indicated that *P. purpureum* fibre has strong potential as a reinforcing material for thermoplastic green composites.

Keywords: Cellulose, crystallinity index, mechanical properties, *Pennisetum purpureum* fibre, scanning electron microscopy, thermogravimetric analysis, X-ray diffraction

INTRODUCTION

Future generations will confront substantial hazards, including global warming, excessive emissions, and the lack of natural resources (Kamaruddin et al., 2021). The extensive reliance on petroleum-based plastics in everyday life has led to serious environmental problems, especially when managing waste (Diyana, Jumaidin, Selamat, Ghazali, et al., 2021). These materials do not decompose readily in nature, whether they are deposited on land or in the ocean, resulting in significant issues for civilisation, wildlife, and the ecosystem. Consequently, the need for more ecologically sustainable materials is significantly rising to protect the environment and maintain ecosystem equilibrium. Finding eco-friendly materials made from renewable resources offers a sustainable alternative to synthetic materials. This approach helps conserve the planet's resources while reducing environmental impact. In recent decades, natural fibres have become increasingly popular due to their unique characteristics, including biodegradability, abundant availability, affordability, non-toxicity, low density, environmental friendliness, recyclability, and excellent balance of strength and weight (Jumaidin et al., 2020; Kamaruddin et al., 2021; Tarique et al., 2021). The increasing demand for traditional fibres, coupled with their limited production, has driven the exploration of new natural fibres made up of cellulose, hemicellulose, lignin, wax, ash, and other soluble compounds (Karimah, Ridho, Munawar, Adi, et al., 2021).

Cellulose is a type of linear polysaccharide made up of glucose molecules. Natural fibres with high cellulose content tend to be stronger and more stable (Tarique et al., 2021). To understand whether a new natural fibre is more crystalline or amorphous, researchers usually calculate its crystallinity index (CI). Natural fibres' properties - physical, mechanical, and chemical—can vary greatly depending on their chemical composition, how mature they are, the part of the plant they come from, the region where the plant was grown, soil nutrient levels, and climate conditions (Biradar et al., 2023).

The importance of natural fibres is highlighted through a comprehensive review of existing research in the same study. A prior study found that the fibre's cellulose levels and the index of crystallinity directly influenced their properties. Natural fibres are often incorporated into composite materials to improve their strength and overall performance (Khalid et al., 2021). Its cellulose content and CI greatly influence the effectiveness of a fibre. These factors play a key role in determining the fibre's performance. The balance between crystalline cellulose and the more amorphous components, like hemicellulose, lignin, and wax, varies depending on the plant's growth environment and conditions. Characteristics of polymer composites depend on various parameters, such as the type of resin, alignment with respect to the respective fibres, and strong bonding between the fibres and the matrix (Chakravarthy K et al., 2020).

Pennisetum purpureum, commonly referred to as Napier grass, is a vital fodder crop in humid tropical regions, valued for its exceptional dry matter production per unit area, surpassing many other grass species. It is extensively cultivated across tropical climates, particularly in Southeast Asia, where annual rainfall typically reaches around 1,000 mm (Onjai-uea et al., 2023). *Pennisetum purpureum* exhibits the ability to thrive in soil conditions that are unfavourable for numerous plant species (Purba & Paengkoum, 2019). *Pennisetum purpureum* exhibits vegetative propagation and possesses the ability to endure many cuttings while swiftly regenerating. This characteristic enables it to yield highly desirable fodder for cattle, particularly in terms of foliage content (Onjai-uea et al., 2023).

The plant's age typically determines the optimal timing for defoliation to ensure maximum production and quality, and recommended guidelines can vary accordingly. For maximum results and high-quality feed, it is recommended to defoliate the grass every 70 days or when the plant reaches a height of 120-150 cm (Chuwongpanich et al., 2019). In addition, it has been proposed by the researcher that grass should be defoliated between 60 and 85 days of age (Ferreira et al., 2019). However, it has also been noted that the harvesting period of the grass can be done after 25 to 30 days during the wet season, or 50 to 60 days during the dry season (Onjai-uea et al., 2023). Meanwhile, increasing the cutting interval to 45 to 60 days will lead to a greater amount of dry matter produced compared to cutting every 30 days (Zaini et al., 2021). The investigations found that as the plant matured, it produced more dry matter, but the overall quality of the plant declined. It indicated that the different harvesting ages of *P. purpureum* resulted in notable variations in the chemical properties of the grass biomass. Grass harvested at a later age contained higher levels of the components that are difficult to degrade, such as lignin. Both the initial features and degradability were altered using a separate method (Chanpla et al., 2018).

A study explored natural fibres, focusing on their thermal, mechanical, and morphological properties, along with their chemical composition (Imraan et al., 2023; Sunny & Rajan, 2022). The impact of betel nut husk (BNH) at different stages of maturity

(raw, ripe, and fully matured) on its mechanical, physical, thermal, and morphological properties was investigated (Sunny & Rajan, 2022). The study revealed that fibres from the ripe stage had the highest tensile strength. On the other hand, sugar palm fibres have been characterised in terms of their tensile and thermal properties, where the maximum tensile strength is found in natural fibre comparison, which attained an ideal chemical composition belonging to that category, featuring a high concentration of cellulose, along with hemicellulose and lignin (Imraan et al., 2023).

While research has explored lignocellulosic fibres as strengthening agents in composite materials, no studies have specifically examined natural cellulosic fibres and the properties of *P. purpureum* fibre based on their optimal harvesting age. This study aimed to analyse the chemical, physical, mechanical, and thermal properties of *P. purpureum* at different fibre ages, comparing them to other well-known natural fibres. The results aim to enhance our understanding of how this natural fibre can be used in various biodegradable products. Despite its potential, there has been limited research on the use and applications of *P. purpureum* fibre and its composites. This study examined the fibre's properties through tests measuring density, chemical composition, mechanical strength, thermal stability, morphology, and functional groups. The findings were then contrasted with other natural fibres.

EXPERIMENTAL METHODS

Raw Materials Preparation

The *P. purpureum grass* was sourced from Ladang Napier Selatan in Rembau, Negeri Sembilan, Malaysia. The fibres were chosen based on the three typical harvesting ages of *P. purpureum grass*, which were 30, 45, and 60 days (Onjai-uea et al., 2023; Zaini et al., 2021).

Fibres Preparation

The surface of the harvested *P. purpureum* grass was washed with clean water to remove any dirt or unwanted particles. The cleaned stems were submerged in fresh water for 14 days to undergo retting, a process that uses microbial activity to break down the plant material. The tank's materials were regularly assessed to confirm that fibres were sufficiently loosened for extraction. After the retting process, the fibres were carefully extracted from the stems by hand. The extracted fibres were rinsed with distilled water to remove any dust, then sun-dried for 48 hr. Afterwards, the fibres were oven-dried at 85°C for an additional 24 hr to eliminate any remaining moisture (Huzaifah et al., 2017). The dried stems were subsequently split into smaller segments prior to the grinding procedure that yielded *P. purpureum* fibre. The water retting flow mechanisms are illustrated in Figures 1(a) to (f).

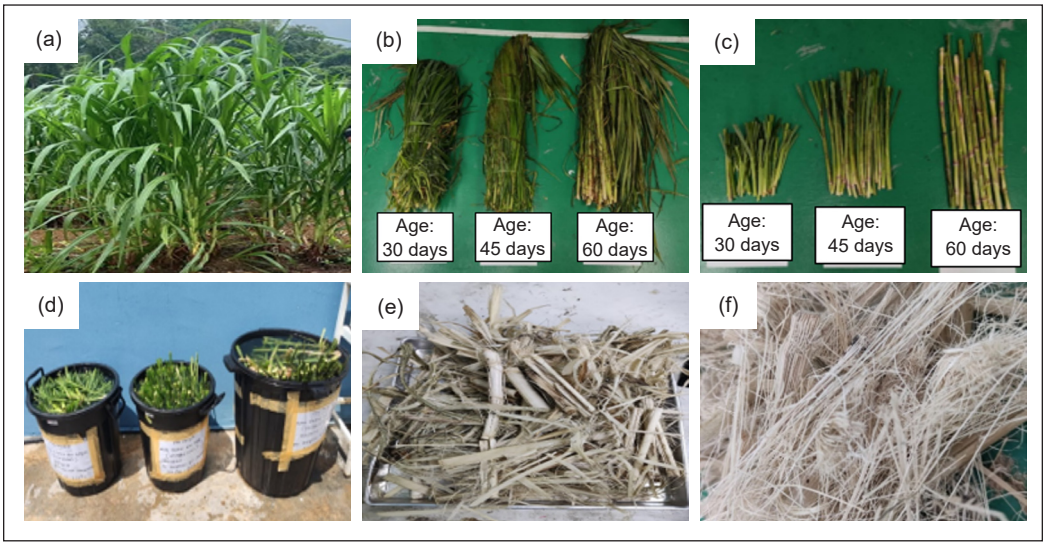

Figure 1. (a) *Pennisetum purpureum* plant; (b) *Pennisetum purpureum* selected at three harvesting ages: 30, 45, and 60 days; (c) cleaned stem; (d) water retting of *Pennisetum purpureum*; (e) dried *Pennisetum purpureum*; and (f) extracted fibres

Chemical Composition

The chemical composition of *P. purpureum* fibre was assessed through neutral detergent fibre (NDF), acid detergent fibre (ADF), and acid detergent lignin (ADL) in accordance with the ISO 13906:2008 standard. The calculated weight percentages of cellulose and hemicellulose were determined using Equations 1 and 2, respectively:

$$\text{Cellulose} = \text{ADF} - \text{ADL} \quad [1]$$

$$\text{Hemicellulose} = \text{NDF} - \text{ADF} \quad [2]$$

Physical Properties

Diameter

The diameter of *P. purpureum* fibres was measured using a Zeiss optical microscope (Axiovert 200, Carl Zeiss Light Microscopy, Germany), analysing 15 individual fibre samples (Kamaruddin et al., 2021). The average diameter was calculated by measuring three different points on each photograph and calculating the mean value (Razali et al., 2015).

Density

The fibre density of *P. purpureum* was determined using an AccuPyc 1340 TEC pycnometer (Micromeritics Instrument Corporation, USA). The pycnometer was used to determine the volume and density of powdered fibre, following ASTM D792 (ASTM International,

2020b), as outlined by Kamaruddin et al. (2021). Helium gas was employed at a constant temperature for this experiment. For each sample, three individual measurements were taken, and the average value was calculated for the data analysis (Ilyas et al., 2017).

Moisture Content

Moisture content was evaluated using five samples, which were dried in an oven at 105°C for 24 hr. To determine the moisture content, the initial weight before drying (Mi, g) and the final weight after drying (Mf, g) were recorded (Diyana, Jumaidin, Selamat, Alamjuri, et al., 2021; Ilyas et al., 2017; Kamaruddin et al., 2021). The moisture content of *P. purpureum* fibre was determined using Equation 3:

$$\text{Moisture content} = \frac{\text{Mi} - \text{Mf}}{\text{Mi}} \times 100\% \qquad [3]$$

Tensile Properties – Single Tensile Test

The ASTM C1557 (ASTM International, 2020a) guideline was utilised for assessing the tensile qualities of *P. purpureum* fibre using a universal testing machine equipped with a 1 kN load cell (Engelbrecht-Wiggans & Forster, 2023). Experiments were conducted with a 25 mm gauge length and a crosshead speed of 1 mm/min. *Pennisetum purpureum* fibre was meticulously selected using an optical microscope before testing to ensure the fibres were undamaged (Razali et al., 2015). Each fibre was secured to the sample holder, and 15 samples were utilised for the assessment of tensile properties, as shown in Figure 2.

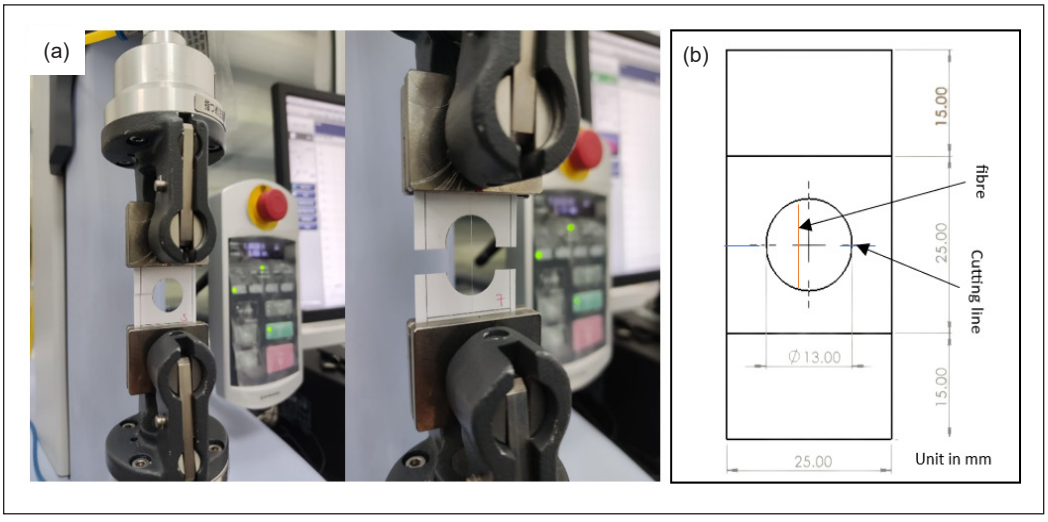

Figure 2. (a) Preparation of samples for tensile testing; and (b)Top-view arrangement of the sample during tensile testing

Thermal Characterisation

Thermogravimetric Analysis (TGA)

To evaluate the thermal stability of *P. purpureum* fibre, a thermogravimetric analyser from TA Instruments (Mettler-Toledo AG, Switzerland) was used, as part of the Thermal Analysis Q series, to determine the fibres' potential for high-temperature applications. A measured amount of *P. purpureum* fibres was placed in an alumina crucible and positioned in a heating chamber. The study was performed inside a nitrogen chamber at a temperature control of 25°C and gradually increased to 900°C at a steady and regular rate of 10°C per minute (Kamaruddin et al., 2021).

Scanning Electron Microscopy (SEM)

The cross-section and morphology of *P. purpureum* fibres were analysed using a Hitachi S-3400N scanning electron microscope (Japan) at an acceleration voltage of 15 kV. Before analysis, the fibres were coated with a thin layer of gold to enhance the imaging. The specimens were 50 mm in length, and the results were obtained through imaging at various magnification levels (Arul Marcel Moshi et al., 2020).

Fourier Transform Infrared Spectroscopy (FTIR)

FTIR spectroscopy was used to analyse all samples and identify the functional groups present in *P. purpureum* fibre. The analysis was carried out with an IR spectrometer (Nicolet 6700 AEM, Thermo Nicolet Corporation, USA). Fine powders were mixed with potassium bromide (KBr, Mody Chemi-Pharma Limited, India) and ground into a fine powder. The powdered sample of approximately 2 mg was combined with the KBr to make a 1-mm-thick disc. The FTIR spectra were recorded from 4000 to 500 cm^{-1} (Diyana, Jumaidin, Selamat, Alamjuri, et al., 2021).

XRD Analysis

The XRD method was selected to assess the CI and crystalline size of *P. purpureum* fibre, utilising a Rigaku D/max 2500 X-ray powder diffractometer (Rigaku, Japan) operating with copper (Cu) radiation at 40 kV and 30 mA, with a wavelength of 0.15406 nm. A scanning rate of 2°/min was employed to examine the samples within the diffraction angle range of 10 to 40° at room temperature. The CI of *P. purpureum* fibre was calculated using the Segal equation, as stated in Equation 4 (Ilyas et al., 2018).

$$CI = \frac{I_{002} - I_{am}}{I_{002}} \times 100\% \qquad [4]$$

Peak intensities for the amorphous and crystalline components are denoted as I002 and Iam, respectively. The crystallite size (CS) was calculated with the use of Scherrer's formula as shown in Equation 5.

$$CS = \frac{k\lambda}{\beta \cos \theta} \times 100\% \quad [5]$$

In this equation, k = 0.89 is Scherrer's constant, λ = 0.1541 nm is the wavelength of the radiation, β represents the full width at half-maximum of the peak in radians, and θ is the corresponding Bragg angle.

RESULTS AND DISCUSSION

Chemical Composition

Natural fibre consists of three key components: cellulose, hemicellulose, and lignin. Cellulose serves as the main structural framework of the fibre, while hemicellulose and lignin surround the cellulose regions, contributing to the fibre's strength, stiffness, and overall stability (Kabir et al., 2012). Analysing the chemical composition of natural fibres is essential for assessing their mechanical characteristic, especially in strength, as the concentration of different chemical components on the fibre's surface plays a significant role in determining their strength (Arul Marcel Moshi et al., 2020). Table 1 compares the results from the examination of the chemical composition of *P. purpureum* fibre across three distinct fibre ages. The highest cellulose content (approximately 45.9%) was observed at 45 days. Meanwhile, the lowest cellulose content was at 30 days (35.61%). At 60 days, cellulose stated the mid value between 30 and 60 days (38.82%). Hemicellulose remained relatively stable across all ages, with a slight increment from 25.03% at 45 days to 27.38% at 60 days. Lignin content, however, dropped significantly at 45 days (10.08%) from 16.47% at 30 days and rose to 13% by 60 days. Based on current observation, the data highlighted 45 days as the optimal harvesting age for balancing high cellulose and low lignin content. The results were then compared to those of other natural fibres, as shown in Table 1.

At 45 days of age, *P. purpureum* fibres contained 45.90% cellulose, relatively higher compared to other natural fibres, such as *Axonopus compressus* (27.28%) (Wahid et al., 2023), *Hylocereus polyrhizus* (34.45) (Taharuddin et al., 2023), *Cymbopogon citratus* leaves (37.56%) (Kamaruddin et al., 2023), and *Arenga pinnata* (44.53%) (Huzaifah et al., 2017). Meanwhile, the cellulose content for 30 and 60 days was lower than that of the other fibres mentioned. The cellulose content for all fibre ages of *P. purpureum* was lower than that of *Pandanus amaryllifolius* (48.79%) (Diyana, Jumaidin, Selamat, Alamjuri, et al., 2021), kenaf (50-55%) (Abdullah et al., 2020), ramie (68-76%) (Goda et al., 2006; Khoo et al., in press; Maideliza et al., 2017), and roselle (60-64%) (Razali et al., 2015).

Table 1
Comparison of the chemical composition of Pennisetum purpureum *fibre and other natural fibres*

Fibre	Fibre age	Cellulose (% wt/wt)	Hemicellulose (% wt/wt)	Lignin (% wt/wt)	Ash (% wt/wt)	References
Pennisetum purpureum	30-days	35.61	26.63	16.47	2.29	Current study
	45-days	45.90	25.03	10.08	2.61	
	60-days	38.82	27.38	13.00	3.64	
Kenaf	12-weeks	50.25-55.43	32.29-37.73	14.87-17.99	0.38-2.45	Abdullah et al. (2020)
	16-weeks	50.85-56.10	24.14-35.41	14.23-17.97	0.29-1.84	
Ramie	50-days 60-days 70-days	68.60-76.20	13.10-16.70	0.60-0.70	-	Goda et al. (2006); Khoo et al. (in press); Maideliza et al. (2017)
Roselle	3-months	64.50	20.23	10.26	1.25	Razali et al. (2015)
	6-months	60.51	16.27	10.26	1.03	
	9-months	58.63	20.82	7.87	2.08	
Axonopus compressus	-	27.28	29.29	11.14	-	Wahid et al. (2023)
Hylocereus polyrhizus		34.45	-	6.73	17.40	Taharuddin et al. (2023)
Pandanus amaryllifolius	-	48.79	19.95	18.64	-	Diyana, Jumaidin, Selamat, Alamjuri, et al. (2021)
Cymbopogon citratus leaves	-	37.56	29.29	11.14	4.28	Kamaruddin et al. (2021)
Arenga pinnata	-	44.53	10.01	41.97	0.955	Huzaifah et al. (2017)

The elevated cellulose content in the fibre enhanced the mechanical properties (Sheltami et al., 2012). The results in Table 1 show that the cellulose content of *P. purpureum* fibre varied significantly with age, which may account for the differing tensile values observed in mechanical testing, in addition to the impact of fibre diameter. The presence of a considerable amount of amorphous compounds in *P. purpureum* fibre, including hemicellulose, lignin, ash, and waxes, may also exert an influence (Campos et al., 2018).

Physical Properties

Diameter and Density

Table 2 presents the values acquired for *P. purpureum* fibre's diameter. Measuring the diameter is crucial for assessing the fibre's mechanical qualities, particularly tensile strength. The diameter of the *P. purpureum* fibre was measured with an optical microscope, as shown in Figure 3. The average diameters of the fibre over 30, 45, and 60 days were determined to be 68, 138, and 162 µm, respectively, equivalent to those of kenaf (57.8-67.5 µm) (Abdullah et al., 2020), roselle (40-10, 90-120, and 90-150 µm) (Razali et al., 2015), *H. polyrhizus* (0.45 µm)

(Taharuddin et al., 2023), *P. amaryllifolius* (368.57 ± 50.47 µm) (Diyana, Jumaidin, Selamat, Alamjuri, et al., 2021), *C. citratus* (326.67 ± 45.77 µm) (Kamaruddin et al., 2021), and *A. pinnata* (0.40 ± 0.08 µm) (Huzaifah et al., 2017). The physical properties are primarily affected by factors like the fibre's origin, the plant's condition, its age, and the method of extraction (Reddy & Yang, 2005).

Density is a crucial parameter in determining the mass of natural fibres and plays a key role in the overall mass of composite materials made from these fibres. The densities of *P. purpureum* fibre at 30, 45, and 60 days were quantified using a pycnometer (Micromeritics Instrument Corporation, USA) with recorded values of 0.67, 1.03, and 1.23 g/cm³, respectively. These values were comparatively lower than those of other natural fibres, such as ramie (1.44, 1.45, and 1.46 g/cm³) (Goda et al., 2006; Khoo et al., in press;

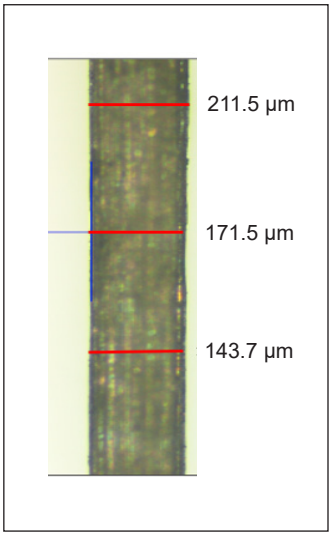

Figure 3. Optical microscopic view of *Pennisetum purpureum* fibre at 100× magnification

Table 2
Comparison of Pennisetum purpureum *fibre's diameter and density with other various fibres*

Fibre	Fibre age	Diameter (µm)	Density (g/cm³)	Moisture content (%)	References
Pennisetum purpureum	30-day	78	0.67	11.06	Current study
	45-day	146	1.03	11.84	
	60-day	159	1.23	11.92	
Kenaf	12-week	57.80-67.50	-	8.33-10.02	Abdullah et al. (2020)
	16-week				
Ramie	50-day	-	1.44	-	Goda et al. (2006); Khoo et al. (in press); Maideliza et al. (2017)
	60-day	-	1.45	-	
	70-day	-	1.46	-	
Roselle	3-month	40-100	1.33	5.80	Razali et al. (2015)
	6-month	80-120	1.42	4.90	
	9-month	90-150	1.42	3.70	
Axonopus compressus	-	-	-	14.95	Wahid et al. (2023)
Hylocereus polyrhizus	-	590	0.45	9.70	Taharuddin et al. (2023)
Pandanus amaryllifolius	-	368.57 ± 50.47	-	6.00 ± 0.13	Diyana, Jumaidin, Selamat, Alamjuri, et al. (2021)
Cymbopogon citratus	-	326.67 ± 45.77	0.25 ± 0.002	5.20 ± 2.28	Kamaruddin et al. (2021)
Arenga pinnata	-	0.40 ± 0.08	1.46 ± 0.012	6.45 ± 1.07	Huzaifah et al. (2017)

Maideliza et al., 2017), roselle (1.44, 1.45, and 1.46 g/cm³) (Razali et al., 2015), *H. polyrhizus* (0.67 g/cm³) (Taharuddin et al., 2023), *C. citratus* (0.25 ± 0.002 g/cm³) (Kamaruddin et al., 2021), and *A. pinnata* (1.46 ± 0.012 g/cm³) (Huzaifah et al., 2017). Table 2 compares the *P. purpureum* fibre's diameter and density with other various fibres. The density of *P. purpureum* fibre highlights its potential for use in the production of low-weight composite materials.

Moisture Content

Moisture content is an essential factor in evaluating a new material for potential reinforcement in composite materials (Kamaruddin et al., 2021). Fibres with low moisture content form a stronger bond with the polymer matrix in composite materials (Jayaramudu et al., 2010). As shown in Table 3, *P. purpureum* fibre of 30, 45, and 60 days age recorded the moisture contents of 11.06, 11.84, and 11.92%, respectively, slightly lower compared to *A. compressus* of 14.95% (Wahid et al., 2023) and slightly higher to the other fibres – kenaf (8.33-10.02%) (Abdullah et al., 2020), roselle (5.80 to 3.70%) (Razali et al., 2015), *H. polyrhizus* (9.70%) (Taharuddin et al., 2023), *P. amaryllifolius* (6.00 ± 0.13%) (Diyana, Jumaidin, Selamat, Alamjuri, et al., 2021), *C. citratus* (5.20 ± 2.28) (Kamaruddin et al., 2021), and *A. pinnata* (6.45 ± 1.07) (Huzaifah et al., 2017). Nevertheless, elevated moisture content demonstrated considerable hydrophilic characteristics. This might show its chemical composition that increased its water adhesivity, making it potentially suitable for high moisture retention applications (Wahid et al., 2023). In summary, the moisture content patterns of *P. purpureum* fibre, in comparison to other natural fibres, underscore its low water retention capacity. This renders it adaptable for medium-stability applications while guaranteeing sufficient mechanical performance. Additional optimisation, including surface treatment, may enhance its functionality in moisture-sensitive settings, expanding its application possibilities.

Tensile Properties

Table 3 presents a comparison of the tensile properties of *P. purpureum* fibre based on fibre age: 30, 45, and 60 days. Maximum strength, which normalises the breaking force relative to the cross-sectional area, showed a different trend. The highest value appeared at 30 days (67.54 MPa), reflecting the fibre's strong tensile capability despite its small diameter. Strength declined significantly to 29.83 MPa at 45 days before rebounding slightly to 41.01 MPa at 60 days. The modulus of elasticity, or stiffness, declined with age, albeit non-linearly. The 30-day fibre exhibited the highest stiffness at 3.14 GPa, indicating it was the least prone to deformation under stress (Zor et al., 2023). By 45 days, the modulus dropped to 1.58 GPa, showing a significant reduction in stiffness, which might be attributed to changes in microfibril angle or structural alignment within the fibre (B. Zhang et al., 2020; Suryanto et al., 2014). At 60 days, the modulus increased to 2.18 GPa, suggesting some recovery of stiffness as the fibre matured (Gallos et al., 2017).

Table 3 also compares the results of tensile properties, strength, and modulus of different ages of *P. purpureum* fibre to those of other well-known natural fibres. The tensile strength of *P. purpureum fibre* depends on factors such as plant age, origin, fibre extraction method, and microstructure. Fibre failure can occur due to cracks forming and spreading from larger imperfections (Bezazi et al., 2014). Therefore, testing at least 15 replicates of each fibre sample is crucial to accurately determine its tensile properties. The remarkable tensile strength of natural fibres is primarily attributed to their high cellulose content and CI (Gurukarthik Babu et al., 2019). The tensile strength of *P. purpureum* fibre was lower compared to other natural fibres, such as kenaf (421–424 MPa) (Abdullah et al., 2020), ramie (859.15–1,150.06 MPa) (Goda et al., 2006; Khoo et al., in press; Maideliza et al., 2017), and Roselle (228.57-453.48 MPa) (Razali et al., 2015). Meanwhile, *P. purpureum* fibre demonstrated a higher tensile strength compared to aerial roots of the banyan tree (19.37 MPa) (Ganapathy et al., 2019), oil palm fruit (49 MPa) (Arul Marcel Moshi et al., 2020), and coconut tree leaf sheath (46.40 MPa) (Kulandaivel et al., 2020).

Table 3
Comparison of tensile properties between Pennisetum purpureum *fibre and various natural fibres*

Fibre	Fibre age	Tensile strength (MPa)	Tensile modulus (GPa)	Elongation at break (%)	References
Pennisetum purpureum	30-day	67.54	3.14	3.46	Current study
	45-day	29.83	1.58	3.38	
	60-day	41.01	2.18	3.03	
Kenaf	12-week	421	-	-	Abdullah et al. (2020)
	16-week	424	-	-	
Ramie	50-day	1,150.06	66.49	1.82	Goda et al. (2006); Khoo et al. (in press); Maideliza et al. (2017)
	60-day	1,089.95	± 57.00	± 1.40	
	70-day	859.15	54.56	1.36	
Roselle	3-month	453.48	-	-	Razali et al. (2015)
	6-month	247.28	-	-	
	9-month	228.57	-	-	
Pandanus amaryllifolius	-	45.61 ± 16.09	0.41 ± 0.18	8.17 ± 3.84	Diyana, Jumaidin, Selamat, Alamjuri, et al. (2021)
Cymbopogon citratus	-	43.81 ± 15.27	1.05 ± 0.33	0.84 ± 0.28	Kamaruddin et al. (2021)
Arenga pinnata	-	233.00 ± 71.17	4.19 ± 1.61	20.6 ± 9.29	Huzaifah et al. (2017)
Aerial roots of the banyan tree	-	19.37	1.80	1.80	Ganapathy et al. (2019)
Coconut tree leaf sheath	-	46.40	2.30	2.84	Kulandaivel et al. (2020)
Oil palm fruit	-	49	2.76	7	Arul Marcel Moshi et al. (2020)

Numerous studies have demonstrated that higher cellulose content and crystallinity typically correlate with greater tensile strength (Kamaruddin et al., 2021; Todkar & Patil, 2019). However, an excessive cellulose content can negatively impact tensile properties due to the inherently hydrophilic nature of cellulose. To further enhance mechanical strength with increased fibre loading, the use of a compatibiliser is recommended (Todkar & Patil, 2019). In general, from the results, despite having the lowest cellulose content (35.61%), the *P. purpureum* fibre at 30 days exhibited the highest tensile strength (67.54 MPa) and tensile modulus (3.14 GPa), likely due to its elevated lignin content (16.47%). Lignin provides structural reinforcement, contributing to the fibre's stiffness and strength (Karimah, Ridho, Munawar, Ismadi, et al., 2021). At 45 days, although the fibre reached its peak cellulose content (45.90%), it showed the lowest tensile strength (29.83 MPa) and modulus (1.58 GPa). This decline in mechanical properties was likely due to a significant reduction in lignin content (10.08%), which played a crucial role in binding cellulose fibrils and providing rigidity (Dorez et al., 2014; Oladele et al., 2020; Sultana, 2014). By 60 days, while cellulose content decreased to 38.82%, both tensile strength and modulus improved compared to 45 days. This improvement correlated to the increase in lignin content (13.00%), indicating that lignin compensated for the lower cellulose levels by enhancing the fibre's rigidity and resistance to deformation (Zor et al., 2023).

The mechanical properties of *P. purpureum* fibres are affected by the intricate relationship between their chemical composition and microstructural features. Although cellulose is essential in influencing tensile strength and modulus, the findings suggested that lignin content and its interplay with cellulose are of similar significance. This has underscored the necessity for a comprehensive approach to assessing fibre performance, considering both chemical composition and structural configuration. Subsequent research may concentrate on analysing cellulose crystallinity and fibre morphology to enhance comprehension of these correlations.

Thermogravimetric Analysis (TGA)

Natural fibres exhibit restricted thermal stability at elevated temperatures, which poses a challenge to their use as reinforcing materials in structural composites (Kamaruddin et al., 2021). Figure 4 illustrates the TGA and derivative thermogravimetric (DTG) curves for *P. purpureum* fibres at three different ages. This thermal analysis evaluates weight loss as the material undergoes heating. As shown in Table 4, three distinct phases of degradation were evident: an initial minor weight loss within 30–102°C, a significant weight loss between 276–390°C, and a final degradation stage extending to the maximum temperature.

The initial phase took place with weight losses of 10.89, 4.78, and 9.29% for fibres aged 30, 45, and 60 days, respectively. This phase was associated with the release of absorbed moisture, a characteristic of the hydrophilic properties of lignocellulosic materials

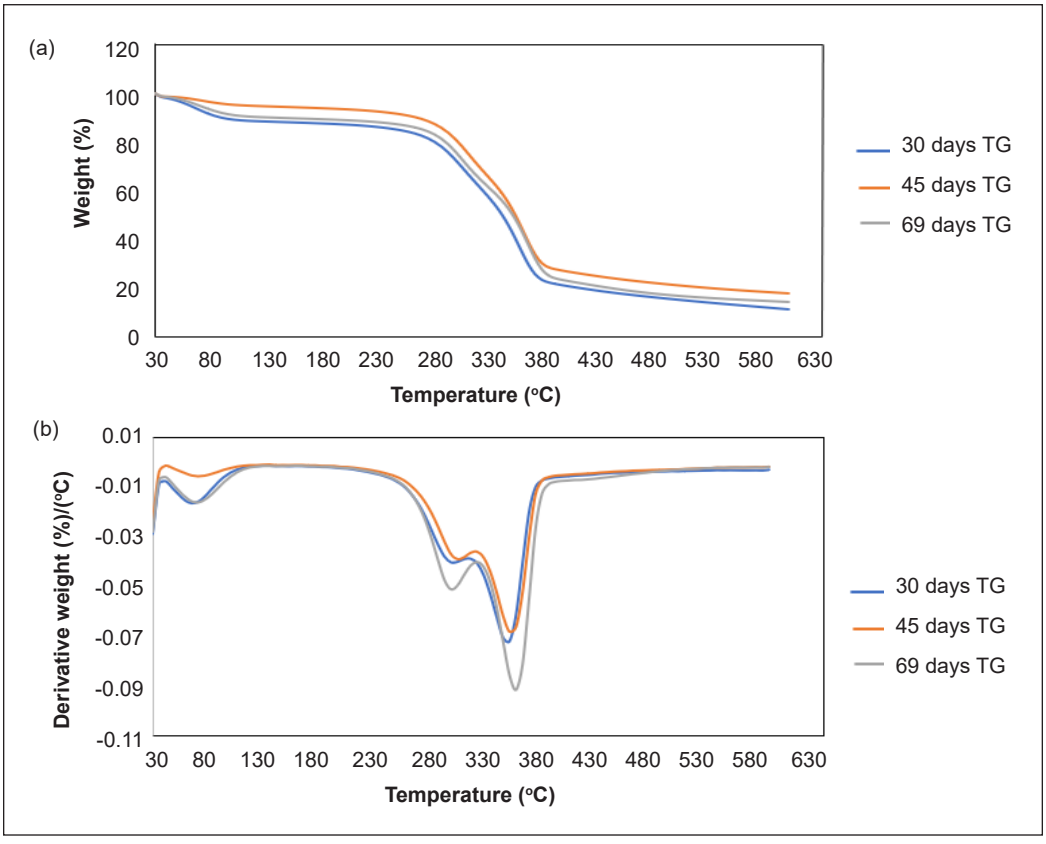

Figure 4. Thermogravimetric (TG) and derivative thermogravimetric (DTG) curves for *Pennisetum purpureum* fibres at various ages: (a) TG curve; and (b) DTG curve

(Boumediri et al., 2019; Mohammed et al., 2023). Subsequently, the fibres demonstrated thermal stability up to around 270°C, as indicated by the absence of notable peaks in both the TGA and DTG curves, which aligned with previous studies (Maache et al., 2017).

The second phase marked a significant weight loss—55.77, 58.40, and 58.99% for fibres aged 30, 45, and 60 days, respectively—resulting from the decomposition of cellulose and hemicellulose. This degradation occurred between 276–378°C, with DTG peak temperatures observed at 378°C for the 30- and 45-day fibres, and at 390°C for the 60-day fibre. This shift in peak temperature suggested the thermal decomposition of cellulose I and the completion of α-cellulose degradation (Abera et al., 2020).

The final degradation phase involved the fragmentation of waxy substances like lignin between 420–500°C, resulting in minor weight losses of 9.87, 8.28, and 7.54% for the respective fibre ages. At the end of the thermal process (600°C), char residue amounted to 23.47, 28.54, and 24.18% for the 30-, 45-, and 60-day fibres, respectively. The char residue primarily consists of carbon or carbon-based materials that resist further thermal

decomposition and remain as residue. Additionally, the presence of inorganic components may contribute to this residue, enabling quantitative estimations of fibre composition (Diyana, Jumaidin, Selamat, Alamjuri, et al., 2021). According to Boumediri et al. (2019), the char residue for *Juncus effusus* L. fibres was found to be 3.64%, while date palm fibres had a char residue of 18.29%. Table 4 shows the thermal degradation of *P. purpureum* fibre at different ages. The thermal stability of *P. purpureum* was comparable with other well-known natural fibres, as shown in Table 5.

Table 4
Thermal degradation properties of Pennisetum purpureum *fibre at different ages*

Sample age (day)	1st thermal degradation			2nd thermal degradation			3rd thermal degradation			Char residue (wt%)
	*T*1 (°C)	Weight loss (%)	*T*peak (°C)	*T*2 (°C)	Weight loss (%)	*T*peak (°C)	*T*3 (°C)	Weight loss (%)	*T*peak (°C)	
30	30 to 102	10.89	102	276 to 378	55.77	378	378 to 540	9.87	504	23.47
45	36 to 102	4.78	84	276 to 378	58.40	378	378 to 480	8.28	492	28.54
60	30 to 102	9.29	102	282 to 390	58.99	390	390 to 510	7.54	510	24.18

Table 5
Degradation temperature of various natural fibres

Natural fibre	Decomposition temperature, initial (°C)	Decomposition temperature, maximum (°C)	References
Pennisetum purpureum fibre – age 30 days	276	378	Current study
Pennisetum purpureum fibre – age 45 days	276	378	Current study
Pennisetum purpureum fibre – age 60 days	282	390	Current study
Axonopus compressus	228	360	Wahid et al. (2023)
Hylocereus polyrhizus	204	306	Taharuddin et al. (2023)
Pandanus amaryllifolius	220	370	Diyana, Jumaidin, Selamat, Alamjuri, et al. (2021)
Cymbopogon citratus	230	338	Kamaruddin et al. (2023)
Sugar palm	228	312	Huzaifah et al. (2017)

Morphological Properties

The morphology of natural fibres is a crucial aspect affecting their mechanical and physical properties, determining their appropriateness as reinforcing materials for composites (Kamaruddin et al., 2021). The SEM pictures illustrate the surface morphology of *P. purpureum* fibres at three distinct growth stages. Figure 5 shows the data for (a) 30 days, (b) 45 days, and (c) 60 days.

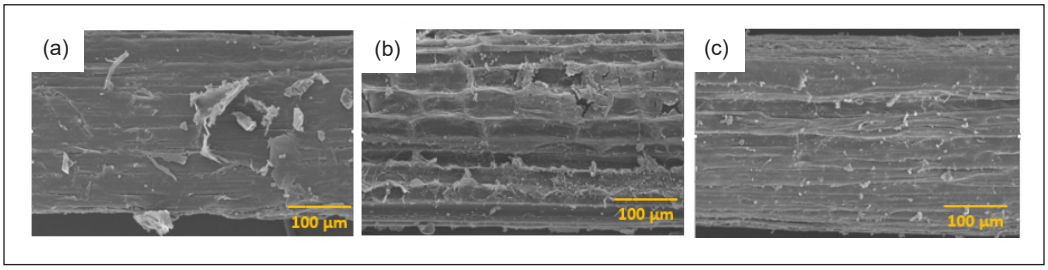

Figure 5. SEM micrographs of *Pennisetum purpureum* raw fibres at different ages: (a) 30 days; (b) 45 days; and (c) 60 days, recorded at 500× magnification with a 100 µm scale bar

At 30 days of fibre age, the surface exhibited a rough texture with several protruding fragments and loose particles. The visible flake-like features suggested incomplete formation or weak bonding of the cell wall layers at this early growth stage. These irregularities were likely due to the relatively high moisture content and the presence of non-fibrous elements, like hemicellulose and pectin, which were still abundant (Radakisnin et al., 2020). The 45-day fibre age showed a more compact and layered structure. The fibre's surface appeared to have fewer fragments than the 30-day sample, indicating ongoing cell wall maturation and deposition of lignin and cellulose (Radakisnin et al., 2020; W. Zhang et al., 2020; Yuan et al., 2024). The 60-day fibre age demonstrated the smoothest and most well-structured morphology. The layers were densely packed with minimal visible defects or loose debris (Radakisnin et al., 2020; Yuan et al., 2024). This aligned with the findings of Diyana, Jumaidin, Selamat, Alamjuri, et al. (2021) and Donaldson et al. (2016), which may be ascribed to the architecture consisting of microfibrils that were tightly arranged and interconnected by lignin, pectin, and other non-cellulosic substances. The architecture of microfibrils was observable and further substantiated the existence of lignin, which bound cellulose microfibrils and safeguarded the structure (Diyana, Jumaidin, Selamat, Alamjuri, et al., 2021).

FTIR Analysis

The FTIR spectra were derived from *Pennisetum purpureum* fibres of varying ages—30, 45, and 60 days. As illustrated in Figure 6, the key peak positions revealed the fibre's composition and the presence of its chemical functional groups. Figure 6 reveals a peak at 3287 cm^{-1} for 30-day aged fibre, showing evidence of O-H bonds in the carboxylic acid group of cellulose components (Ilaiya Perumal & Sarala et al., 2020; Vijay et al., 2020). The following two peaks of *P. purpureum* fibre, found at 2917 and 2850 cm^{-1}, were associated with the C-H stretching vibrations of CH and CH_2 groups, which alluded to the cellulose and hemicellulose presence (Ilyas et al., 2017; Kulandaivel et al., 2020). A peak at 2000 cm^{-1} was linked to the symmetrical stretching of CH_2 in wax, while a smaller peak at 1641 cm^{-1} was associated with the hemicellulose components (Gurukarthik Babu et al.,

2019). The peak at 1517 cm^{-1} captured a minute amount of moisture presence, while the peak at 1033 cm^{-1} was linked to lignin, specifically the C-OH molecules (Manimaran et al., 2020). The presence of absorption bands around 1030–1033 cm^{-1} across all spectra corresponds to the C–O–C stretching vibrations within the pyranose ring, indicative of polysaccharide structures such as cellulose and hemicellulose. This assignment aligns with characteristic infrared bands observed in polysaccharides, where the C–O–C stretching vibrations typically appear in this region (Gieroba et al., 2023). However, the absence of a distinct peak in the 900–950 cm^{-1} range suggests that the C–O.–C glycosidic bond vibrations are not prominently featured in the spectra (Das et al., 2024). Table 6 compares FTIR peak positions and the stretching vibration patterns in *P. purpureum* fibres at the ages of 30, 45, and 60 days.

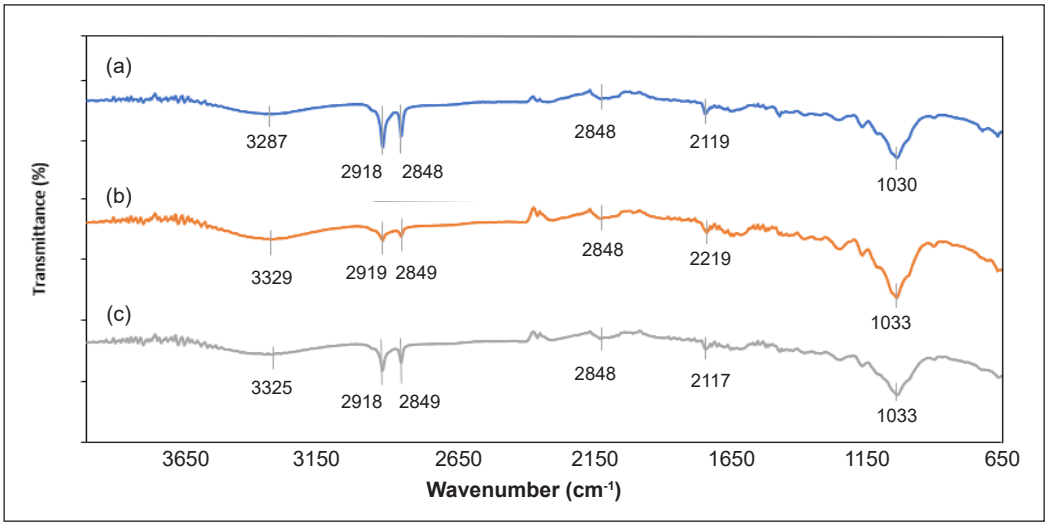

Figure 6. Fourier transform infrared spectroscopy spectrum analyses for *Pennisetum purpureum* fibre for different fibre ages: (a) 30-day; (b) 45-day; and (c) 60-day

Table 6
FTIR peak locations and chemical stretching allocations of Pennisetum purpureum for 30, 45, and 60 days of fibre

Allocations	Fibre age		
	Wavenumber (cm^{-1})		
	30-day	45-day	60-day
OH stretching in α-cellulose	3287	3329	3325
CH stretching in α-cellulose	2918 and 2848	2919 and 2849	2918 and 2849
C=C stretching in wax	2119	2129	2117
C=O stretching in hemicellulose	1731	1728	1734
C-OH vibration in lignin	1030	1033	1033

XRD Analysis

Figure 7 illustrates the X-ray diffractogram for *P. purpureum* fibres at three different ages. The XRD spectra of *P. purpureum* fibres revealed two clear peaks at around 2θ = 16.14° and 22.02° for the 30-day fibres, 16.41° and 22.3° for the 45-day fibres, and 16.39° and 22.3° for the 60-day fibres. The initial peak, located around the 16.14° diffraction angle, corresponded to the components of amorphous presence in *P. purpureum* fibre. The subsequent peak revealed the crystalline component in *P. purpureum*. The elevated CI observed in *P. purpureum* fibre demonstrated superior mechanical capabilities and molecular organisation (Indran et al., 2014). The sharpness of the diffraction peaks reflected the degree of crystallinity, with sharper peaks indicating greater crystallinity in the fibre (Alemdar & Sain, 2008). The CI of *Pennisetum purpureum* fibre was calculated using the Segal empirical technique, as indicated in Equation 4, yielding values of 51.19, 49.40, and 50.56% for fibre ages of 30, 45, and 60 days, respectively. The crystalline sizes were estimated to be 1.68 nm for 30-day age, 1.26 nm for 45-day age, and 1.83 nm for 60-day age. The elevated CI at 30 days, despite a reduced cellulose content relative to the 45-day fibre, can be attributed to the gradual reduction of amorphous constituents such as hemicellulose and lignin. While cellulose is the principal factor in crystallinity, the elimination or degradation of hemicellulose and lignin during plant maturation enhanced the packing density and arrangement of the residual cellulose chains. French (2014) emphasized that less amorphous content promotes the development of more defined crystalline areas in cellulose. Furthermore, lignin enhances the structural rigidity of the fibre matrix, facilitating the alignment of cellulose chains, whilst the semi-crystalline characteristics of hemicellulose assist in integrating cellulose microfibrils into a cohesive structure. These interactions create a stable environment for the formation of crystalline areas in cellulose, notwithstanding the moderate cellulose content. Comparable results

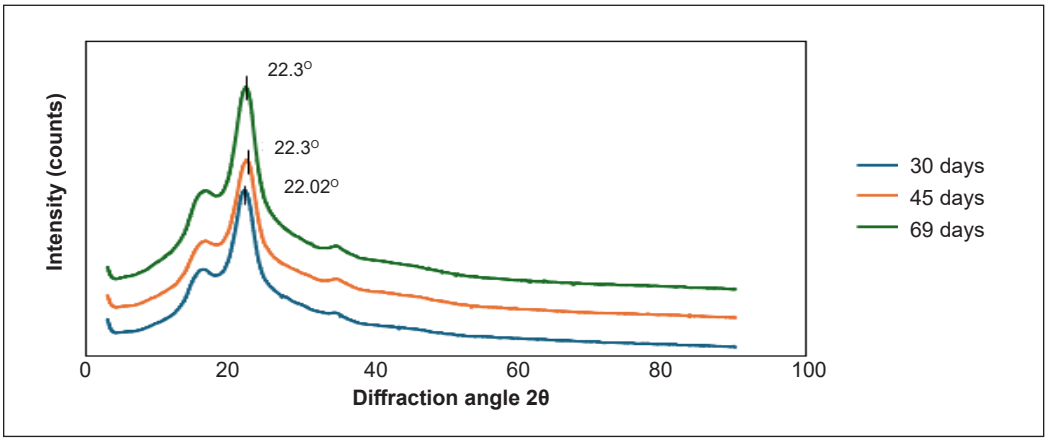

Figure 7. X-ray diffraction trends of *Pennisetum purpureum* fibre for different ages: 30, 45, and 60 days

were documented by Mazumder and Zhang (2023), who observed that the interactions of lignin and hemicellulose with cellulose are crucial for improving crystalline organisation during the initial stages of fibre development.

The CI value of *P. purpureum* fibre surpassed that of most natural fibres, including *H. polyrhizus* (32.76%), *P. amaryllifolius* (37.09%), *C. citratus* (35.2%), *Tridax procumbens* (34.46%), and *J. effusus* L. (33.40%), yet was marginally lower than that of *Pandanus tectorius* (55.10%) and *Cissus quadrangularis* root, as presented in Table 7. Consequently, the crystallinity value was contingent upon the cellulose concentration and the plant species. There exist correlations among fibre stiffness, the degree of crystallinity, and cellulose concentration. Enhancing the crystallinity area augmented the stiffness of the fibres; this can be associated with the correlation of increased fibre crystallinity and cellulose content (Kamaruddin et al., 2021). X-ray diffraction analysis indicated that *P. purpureum* fibre could be a promising material for reinforcing polymer composites.

Table 7
Comparison of the crystallinity of Pennisetum purpureum *fibre and other various fibres*

Fibre	Crystallinity index (%)	Crystallinity size (nm)	References
Pennisetum purpureum - age 30 days	51.19	1.68	Current study
Pennisetum purpureum - age 45 days	49.40	1.26	Current study
Pennisetum purpureum - age 60 days	50.56	1.83	Current study
Hylocereus polyrhizus	32.76		Taharuddin et al. (2023)
Pandanus amaryllifolius	37.09	4.95	Diyana, Jumaidin, Selamat, Alamjuri, et al. (2021)
Cymbopogon citratus	35.2	-	Kamaruddin et al. (2021)
Tridax procumbens	34.4	25.04	Garette Jebadurai et al. (2019)
Juncus effusus L.	33.40	3.60	Narayanasamy et al. (2020)
Ficus religiosa	42.92	5.18	Chakravarthy K et al. (2020)
Pandanus tectorius	55.10	-	Narayanasamy et al. (2020)
Cissus quadrangularis root	56.60	7.04	Balaji and Nagarajan (2017)

CONCLUSION

This study highlighted that fibres from *P. purpureum* at three different ages (30, 45, and 60 days) were successfully extracted using a water-retting process specific to each age group. These fibres were subsequently analyzed to evaluate their physical, mechanical, thermal, and chemical properties. The density of *P. purpureum* fibre varies with age, influencing its suitability for different applications. The fibres at 30, 45, and 60 days recorded densities of 0.67, 1.03, and 1.23 g/cm^3, respectively, which are lower than many other natural fibres, such as ramie, roselle, and *A. pinnata*. This relatively low density suggests that *P.*

purpureum fibres could be advantageous in producing lightweight composite materials. The fibre of *P. purpureum* showed significant changes in chemical composition depending on the harvesting age. The mechanical properties of *P. purpureum* fibres were not solely dependent on cellulose content but were greatly influenced by the balance and interaction between cellulose and lignin. The optimal mechanical performance at 30 days highlighted the critical role of lignin in providing structural reinforcement (tensile strength: 67.537 MPa, modulus: 3.142 GPa, cellulose: 35.61%, and lignin: 16.47%). The density of the *P. purpureum* fibre increased significantly with age (30, 45, and 60 days), suggesting increased lignification and cell wall compaction over time. Meanwhile, moisture content increased slightly with age, reflecting a potential increase in hydrophilic components like hemicellulose. Thermogravimetric analysis indicated that fibre age influences thermal degradation, with older fibres showing more hemicellulose decomposition and better thermal stability. The 45-day fibre exhibited the lowest moisture loss (4.78%) and the highest char residue (28.54%), indicating better thermal resistance compared to the 30-day and 60-day fibres. The major weight loss due to cellulose and hemicellulose decomposition occurred between 276–390°C, with the 60-day fibre showing a slightly higher peak degradation temperature (390°C), suggesting a more structured cellulose composition. The consistent char residue suggested that the fibres have the potential for applications requiring high thermal resistance. The XRD analysis of *P. purpureum* fibres at different ages revealed distinct crystalline and amorphous regions, with two major peaks appearing consistently around 16° and 22°. The CI values for fibres aged 30, 45, and 60 days were 51.19, 49.40, and 50.56%, respectively, indicating that fibre age influences the crystalline structure. The highest CI value at 30 days suggests that the reduction of amorphous components, such as hemicellulose and lignin, contributed to better molecular organization. Despite variations in cellulose content, the alignment of cellulose chains and interactions with lignin and hemicellulose played a crucial role in enhancing the crystalline structure. This study will be expanded to assess the compatibility of *P. purpureum* fibre with a biodegradable matrix sourced from natural materials.

ACKNOWLEDGEMENTS

The authors would like to thank Universiti Teknikal Malaysia Melaka, Universiti Malaysia Sabah, Universiti Kuala Lumpur, and the Ministry of Higher Education Malaysia for the financial support through the research grant FRGS/1/2023/STG05/UTEM/02/2.

REFERENCES

Abdullah, H. H., Zakaria, S., Anuar, N. I. S., Mohd Salleh, K., & Syeed Jaafar, S. N. (2020). Effect of harvesting time and water retting fiber processing methods on the physico-mechanical properties of kenaf fiber. *BioResources*, *15*(3), 7207–7222. https://doi.org/10.15376/BIORES.15.3.7207-7222

Abera, G., Woldeyes, B., Demash, H. D., & Miyake, G. (2020). The effect of plasticizers on thermoplastic starch films developed from the indigenous Ethiopian tuber crop anchote (*Coccinia abyssinica*) starch. *International Journal of Biological Macromolecules*, *155*, 581–587. https://doi.org/10.1016/j.ijbiomac.2020.03.218

Alemdar, A., & Sain, M. (2008). Isolation and characterization of nanofibers from agricultural residues - Wheat straw and soy hulls. *Bioresource Technology*, *99*(6), 1664–1671. https://doi.org/10.1016/j.biortech.2007.04.029

Arul Marcel Moshi, A., Ravindran, D., Sundara Bharathi, S. R., Padma, S. R., Indran, S., & Divya, D. (2020). Characterization of natural cellulosic fiber extracted from *Grewia damine* flowering plant's stem. *International Journal of Biological Macromolecules*, *164*, 1246–1255. https://doi.org/10.1016/j.ijbiomac.2020.07.225

ASTM International. (2020a). *ASTM C1557-20: Standard test method for tensile strength and Young's modulus of fibers*. https://store.astm.org/c1557-20.html

ASTM International. (2020b). *ASTM D792-20: Standard test methods for density and specific gravity (relative density) of plastics by displacement*. https://store.astm.org/d0792-20.html

Balaji, A. N., & Nagarajan, K. L. (2017). Characterization of alkali treated and untreated new cellulosic fiber from Saharan aloe vera cactus leaves. *Carbohydrate Polymers*, *174*, 200–208. https://doi.org/10.1016/j.carbpol.2017.06.065

Bezazi, A., Belaadi, A., Bourchak, M., Scarpa, F., & Boba, K. (2014). Novel extraction techniques, chemical and mechanical characterisation of *Agave americana* L. natural fibres. *Composites Part B: Engineering*, *66*, 194–203. https://doi.org/10.1016/j.compositesb.2014.05.014

Biradar, A., Arulvel, S., & Kandasamy, J. (2023). Significance of ballistic parameters and nanohybridization in the development of textile-based body armor: A review. *International Journal of Impact Engineering*, *180*, 104700. https://doi.org/10.1016/j.ijimpeng.2023.104700

Boumediri, H., Bezazi, A., Del Pino, G. G., Haddad, A., Scarpa, F., & Dufresne, A. (2019). Extraction and characterization of vascular bundle and fiber strand from date palm rachis as potential bio-reinforcement in composite. *Carbohydrate Polymers*, *222*, 114997. https://doi.org/10.1016/j.carbpol.2019.114997

Campos, A., Sena Neto, A. R., Rodrigues, V. B., Luchesi, B. R., Mattoso, L. H. C., & Marconcini, J. M. (2018). Effect of raw and chemically treated oil palm mesocarp fibers on thermoplastic cassava starch properties. *Industrial Crops and Products*, *124*, 149–154. https://doi.org/10.1016/j.indcrop.2018.07.075

Chakravarthy K, S., Madhu S., Raju, J. S. N., & Shariff Md, J. (2020). Characterization of novel natural cellulosic fiber extracted from the stem of *Cissus vitiginea* plant. *International Journal of Biological Macromolecules*, *161*, 1358–1370. https://doi.org/10.1016/j.ijbiomac.2020.07.230

Chanpla, M., Kullavanijaya, P., Janejadkarn, A., & Chavalparit, O. (2018). Effect of harvesting age and performance evaluation on biogasification from Napier grass in separated stages process. *KSCE Journal of Civil Engineering*, *22*(1), 40–45. https://doi.org/10.1007/s12205-017-1164-y

Chuwongpanich, W., Chittamart, N., Tawornpruek, S., Aramrak, S., & Fujii, K. (2019). *Studies on microbial biomass carbon and nitrogen turnover derived from sugarcane residues incorporated into a sandy loam*. ResearchGate. https://www.researchgate.net/publication/338965599_STUDIES_ON_MICROBIAL_

BIOMASS_CARBON_AND_NITROGEN_TURNOVER_DERIVED_FROM_SUGARCANE_RESIDUES_INCORPORATED_INTO_A_SANDY_LOAM_SOIL

Das, S., Bhati, V., Dewangan, B. P., Gangal, A., Mishra, G. P., Dikshit, H. K., & Pawar, P. A. M. (2024). Combining Fourier-transform infrared spectroscopy and multivariate analysis for chemotyping of cell wall composition in mungbean (*Vigna radiata* (L.) Wizcek). *Plant Methods*, *20*, 135. https://doi.org/10.1186/s13007-024-01260-w

Diyana, Z. N., Jumaidin, R., Selamat, M. Z., Alamjuri, R. H., & Md Yusof, F. A. (2021). Extraction and characterization of natural cellulosic fiber from *Pandanus amaryllifolius* leaves. *Polymers*, *13*(23), 4171. https://doi.org/10.3390/polym13234171

Diyana, Z. N., Jumaidin, R., Selamat, M. Z., Ghazali, I., Julmohammad, N., Huda, N., & Ilyas, R. A. (2021). Physical properties of thermoplastic starch derived from natural resources and its blends: A review. *Polymers*, *13*(9), 1396. https://doi.org/10.3390/polym13091396

Donaldson, L., Nanayakkara, B., & Harrington, J. (2016). Wood growth and development. In B. Thomas, B. G. Murray, & D. J. Murphy (Eds.), *Encyclopedia of applied plant sciences* (2nd ed., Vol. 1, pp. 203–210). Academic Press. https://doi.org/10.1016/B978-0-12-394807-6.00114-3

Dorez, G., Ferry, L., Sonnier, R., Taguet, A., & Lopez-Cuesta, J.-M. (2014). Effect of cellulose, hemicellulose and lignin contents on pyrolysis and combustion of natural fibers. *Journal of Analytical and Applied Pyrolysis*, *107*, 323–331. https://doi.org/10.1016/j.jaap.2014.03.017

Engelbrecht-Wiggans, A. E., & Forster, A. L. (2023). Analysis of strain correction procedures for single fiber tensile testing. *Composites Part A: Applied Science and Manufacturing*, *167*, 107411. https://doi.org/10.1016/j.compositesa.2022.107411

Ferreira, E. A., de Abreu, J. G., Martinez, J. C., Amorim, R. S. S., Neto, A. B., Cabral, C. E. A., dos Santos Braz, T. G., Júnior, C. A. S., & Ferreira, D. P. (2019). Productivity and nutritional value of elephant grass BRS Canará forage. *Semina:Ciencias Agrarias*, *40*(6), 2705–2718. https://doi.org/10.5433/1679-0359.2019v40n6p2705

French, A. D. (2014). Idealized powder diffraction patterns for cellulose polymorphs. *Cellulose*, *21*, 885–896. https://doi.org/10.1007/s10570-013-0030-4

Gallos, A., Paës, G., Allais, F., & Beaugrand, J. (2017). Lignocellulosic fibers: A critical review of the extrusion process for enhancement of the properties of natural fiber composites. *RSC Advances*, *7*(55), 34638–34654. https://doi.org/10.1039/c7ra05240e

Ganapathy, T., Sathiskumar, R., Senthamaraikannan, P., Saravanakumar, S. S., & Khan, A. (2019). Characterization of raw and alkali treated new natural cellulosic fibres extracted from the aerial roots of banyan tree. *International Journal of Biological Macromolecules*, *138*, 573–581. https://doi.org/10.1016/j.ijbiomac.2019.07.136

Garette Jebadurai, S., Edwin Raj, R., Sreenivasan, V. S., & Binoj, J. S. (2019). Comprehensive characterization of natural cellulosic fiber from *Coccinia grandis* stem. *Carbohydrate Polymers*, *207*, 675–683. https://doi.org/10.1016/j.carbpol.2018.12.027

Gieroba, B., Kalisz, G., Krysa, M., Khalavka, M., & Przekora, A. (2023). Application of vibrational spectroscopic techniques in the study of the natural polysaccharides and their cross-linking process. *International Journal of Molecular Sciences*, *24*(3), 2630. https://doi.org/10.3390/ijms24032630

Goda, K., Sreekala, M. S., Gomes, A., Kaji, T., & Ohgi, J. (2006). Improvement of plant based natural fibers for toughening green composites - Effect of load application during mercerization of ramie fibers. *Composites Part A: Applied Science and Manufacturing*, *37*(12), 2213–2220. https://doi.org/10.1016/j.compositesa.2005.12.014

Gurukarthik Babu, B., Prince Winston, D., SenthamaraiKannan, P., Saravanakumar, S. S., & Sanjay, M. R. (2019). Study on characterization and physicochemical properties of new natural fiber from *Phaseolus vulgaris*. *Journal of Natural Fibers*, *16*(7), 1035–1042. https://doi.org/10.1080/15440478.2018.1448318

Huzaifah, M. R. M., Sapuan, S. M., Leman, Z., & Ishak, M. R. (2017). Comparative study on chemical composition, physical, tensile, and thermal properties of sugar palm fiber (*Arenga pinnata*) obtained from different geographical locations. *BioResources*, *12*(4), 9366–9382. https://doi.org/10.15376/biores.12.4.9366-9382

Ilaiya Perumal, C., & Sarala, R. (2020). Characterization of a new natural cellulosic fiber extracted from *Derris scandens* stem. *International Journal of Biological Macromolecules*, *165*(Part B), 2303-2313. https://doi.org/10.1016/j.ijbiomac.2020.10.086

Ilyas, R. A., Sapuan, S. M., Ishak, M. R., & Zainudin, E. S. (2017). Effect of delignification on the physical, thermal, chemical, and structural properties of sugar palm fibre. *BioResources*, *12*(4), 8734–8754. https://doi.org/10.15376/biores.12.4.8734-5754

Ilyas, R. A., Sapuan, S. M., Ishak, M. R., & Zainudin, E. S. (2018). Development and characterization of sugar palm nanocrystalline cellulose reinforced sugar palm starch bionanocomposites. *Carbohydrate Polymers*, *202*, 186–202. https://doi.org/10.1016/j.carbpol.2018.09.002

Imraan, M., Ilyas, R. A., Norfarhana, A. S., Bangar, S. P., Knight, V. F., & Norrrahim, M. N. F. (2023). Sugar palm (*Arenga pinnata*) fibers: New emerging natural fibre and its relevant properties, treatments and potential applications. *Journal of Materials Research and Technology*, *24*, 4551–4572. https://doi.org/10.1016/j.jmrt.2023.04.056

Indran, S., Edwin Raj, R., & Sreenivasan, V. S. (2014). Characterization of new natural cellulosic fiber from *Cissus quadrangularis* root. *Carbohydrate Polymers*, *110*, 423–429. https://doi.org/10.1016/j.carbpol.2014.04.051

Jayaramudu, J., Guduri, B. R., & Varada Rajulu, A. (2010). Characterization of new natural cellulosic fabric *Grewia tilifolia*. *Carbohydrate Polymers*, *79*(4), 847–851. https://doi.org/10.1016/j.carbpol.2009.10.046

Jumaidin, R., Khiruddin, M. A. A., Saidi, Z. A. S., Salit, M. S., & Ilyas, R. A. (2020). Effect of cogon grass fibre on the thermal, mechanical and biodegradation properties of thermoplastic cassava starch biocomposite. *International Journal of Biological Macromolecules*, *146*, 746–755. https://doi.org/10.1016/j.ijbiomac.2019.11.011

Kabir, M. M., Wang, H., Lau, K. T., & Cardona, F. (2012). Chemical treatments on plant-based natural fibre reinforced polymer composites: An overview. *Composites Part B: Engineering*, *43*(7), 2883–2892. https://doi.org/10.1016/j.compositesb.2012.04.053

Kamaruddin, Z. H., Jumaidin, R., Kamaruddin, Z. H., Asyraf, M. R. M., Razman, M. R., & Khan, T. (2023). Effect of *Cymbopogon citratus* fibre on physical and impact properties of thermoplastic cassava starch/palm wax composites. *Polymers*, *15*(10), 2364. https://doi.org/10.3390/polym15102364

Kamaruddin, Z. H., Jumaidin, R., Rushdan, A. I., Selamat, M. Z., & Alamjuri, R. H. (2021). Characterization of natural cellulosic fiber isolated from Malaysian *Cymbopogon citratus* leaves. *BioResources*, *16*(4), 7729–7750. https://doi.org/10.15376/biores.16.4.7729-7750

Karimah, A., Ridho, M. R., Munawar, S. S., Adi, D. S., Ismadi., Damayanti, R., Subiyanto, B., Fatriasari, W., & Fudholi, A. (2021). A review on natural fibers for development of eco-friendly bio-composite: Characteristics, and utilizations. *Journal of Materials Research and Technology*, *13*, 2442–2458. https://doi.org/10.1016/j.jmrt.2021.06.014

Karimah, A., Ridho, M. R., Munawar, S. S., Ismadi., Amin, Y., Damayanti, R., Lubis, M. A. R., Wulandari, A. P., Nurindah., Iswanto, A. H., Fudholi, A., Asrofi, M., Saedah, E., Sari, N. H., Pratama, B. R., Fatriasari, W., Nawawi, D. S., Rangappa, S. M., & Siengchin, S. (2021). A comprehensive review on natural fibers: Technological and socio-economical aspects. *Polymers*, *13*(24), 4280. https://doi.org/10.3390/polym13244280

Khalid, M. Y., Al Rashid, A., Arif, Z. U., Ahmed, W., Arshad, H., & Zaidi, A. A. (2021). Natural fiber reinforced composites: Sustainable materials for emerging applications. *Results in Engineering*, *11*, 100263. https://doi.org/10.1016/j.rineng.2021.100263

Khoo, P. S., Hassan, S. A., Ilyas, R. A., Loganathan, T. G., Adhiguna, R. T., Reby Roy, K. E., & Mubarak Ali, M. (in press). Tensile properties of ramie fibre: Effect of harvesting day and extraction method. *Materials Today: Proceedings*. https://doi.org/10.1016/j.matpr.2023.04.247

Kulandaivel, N., Muralikannan, R., & KalyanaSundaram, S. (2020). Extraction and characterization of novel natural cellulosic fibers from pigeon pea plant. *Journal of Natural Fibers*, *17*(5), 769–779. https://doi.org/10.1080/15440478.2018.1534184

Maache, M., Bezazi, A., Amroune, S., Scarpa, F., & Dufresne, A. (2017). Characterization of a novel natural cellulosic fiber from *Juncus effusus* L. *Carbohydrate Polymers*, *171*, 163–172. https://doi.org/10.1016/j.carbpol.2017.04.096

Maideliza, T., Mayerni, R., & Rezki, D. (2017). Comparative study of length and growth rate of ramie (*Boehmeria nivea* L. Gaud.) bast fiber of Indonesian clones. *International Journal on Advanced Science, Engineering and Information Technology*, *7*(6), 2273–2278.

Manimaran, P., Pillai, G. P., Vignesh, V., & Prithiviraj, M. (2020). Characterization of natural cellulosic fibers from Nendran Banana Peduncle plants. *International Journal of Biological Macromolecules*, *162*, 1807–1815. https://doi.org/10.1016/j.ijbiomac.2020.08.111

Mazumder, S., & Zhang, N. (2023). Cellulose–hemicellulose–lignin interaction in the secondary cell wall of coconut endocarp. *Biomimetics*, *8*(2), 188. https://doi.org/10.3390/biomimetics8020188

Mohammed, M., Mohamad Jawad, A. J., Mohammed, A. M., Oleiwi, J. K., Adam, T., Osman, A. F., Dahham, O. S., Betar, B. O., Gopinath, S. C. B., & Jaafar, M. (2023). Challenges and advancement in water absorption of natural fiber-reinforced polymer composites. *Polymer Testing*, *124*, 108083. https://doi.org/10.1016/j.polymertesting.2023.108083

Narayanasamy, P., Balasundar, P., Senthil, S., Sanjay, M. R., Siengchin, S., Khan, A., & Asiri, A. M. (2020). Characterization of a novel natural cellulosic fiber from *Calotropis gigantea* fruit bunch for ecofriendly

polymer composites. *International Journal of Biological Macromolecules*, *150*, 793–801. https://doi.org/10.1016/j.ijbiomac.2020.02.134

Oladele, I. O., Michael, O. S., Adediran, A. A., Balogun, O. P., & Ajagbe, F. O. (2020). Acetylation treatment for the batch processing of natural fibers: Effects on constituents, tensile properties and surface morphology of selected plant stem fibers. *Fibers*, *8*(12), 73. https://doi.org/10.3390/fib8120073

Onjai-uea, N., Paengkoum, S., Taethaisong, N., Thongpea, S., Sinpru, B., Surakhunthod, J., Meethip, W., Purba, R. A. P., & Paengkoum, P. (2023). Effect of cultivar, plant spacing and harvesting age on yield, characteristics, chemical composition, and anthocyanin composition of purple Napier grass. *Animals*, *13*(1), 10. https://doi.org/10.3390/ani13010010

Purba, R. A. P., & Paengkoum, P. (2019). Bioanalytical HPLC method of *Piper betle* L. for quantifying phenolic compound, water-soluble vitamin, and essential oil in five different solvent extracts. *Journal of Applied Pharmaceutical Science*, *9*(5), 33–39. https://doi.org/10.7324/JAPS.2019.90504

Radakisnin, R., Abdul Majid, M. S., Mohd Jamir, M. R., Jawaid, M., Sultan, M. T. H., & Mat Tahir, M. F. (2020). Structural, morphological and thermal properties of cellulose nanofibers from napier fiber (*Pennisetum purpureum*). *Materials*, *13*(18), 4125. https://doi.org/10.3390/ma13184125

Razali, N., Salit, M. S., Jawaid, M., Ishak, M. R., & Lazim, Y. (2015). A study on chemical composition, physical, tensile, morphological, and thermal properties of roselle fibre: Effect of fibre maturity. *BioResources*, *10*(1), 1803–1824. https://doi.org/10.15376/biores.10.1.1803-1824

Reddy, N., & Yang, Y. (2005). Biofibers from agricultural byproducts for industrial applications. *Trends in Biotechnology*, *23*(1), 22–27. https://doi.org/10.1016/j.tibtech.2004.11.002

Sheltami, R. M., Abdullah, I., Ahmad, I., Dufresne, A., & Kargarzadeh, H. (2012). Extraction of cellulose nanocrystals from mengkuang leaves (*Pandanus tectorius*). *Carbohydrate Polymers*, *88*(2), 772–779. https://doi.org/10.1016/j.carbpol.2012.01.062

Sultana, R. S., & Rahman, M. M. (2014). An overview of microfibril angle in fiber of tension wood. *European Journal of Biophysics*, *2*(2), 7-12. https://doi.org/10.11648/j.ejb.20140202.11

Sunny, G., & Rajan, T. P. (2022). Review on areca nut fiber and its implementation in sustainable products development. *Journal of Natural Fibers*, *19*(12), 4747–4760. https://doi.org/10.1080/15440478.2020.1870623

Suryanto, H., Marsyahyo, E., Irawan, Y. S., & Soenoko, R. (2014). Morphology, structure, and mechanical properties of natural cellulose fiber from Mendong grass (*Fimbristylis globulosa*). *Journal of Natural Fibers*, *11*(4), 333–351. https://doi.org/10.1080/15440478.2013.879087

Taharuddin, N. H., Jumaidin, R., Mansor, M. R., Md Yusof, F. A., & Alamjuri, R. H. (2023). Characterization of potential cellulose from *Hylocereus polyrhizus* (dragon fruit) peel: A study on physicochemical and thermal properties. *Journal of Renewable Materials*, *11*(1), 131–145. https://doi.org/10.32604/jrm.2022.021528

Tarique, J., Sapuan, S. M., Khalina, A., Sherwani, S. F. K., Yusuf, J., & Ilyas, R. A. (2021). Recent developments in sustainable arrowroot (*Maranta arundinacea* Linn) starch biopolymers, fibres, biopolymer composites and their potential industrial applications: A review. *Journal of Materials Research and Technology*, *13*, 1191–1219. https://doi.org/10.1016/j.jmrt.2021.05.047

Todkar, S. S., & Patil, S. A. (2019). Review on mechanical properties evaluation of pineapple leaf fibre (PALF) reinforced polymer composites. *Composites Part B: Engineering*, *174*, 106927. https://doi.org/10.1016/j.compositesb.2019.106927

Vijay, R., Singaravelu, D. L., Vinod, A., Paul Raj, I. D. F., Sanjay, M. R., & Siengchin, S. (2020). Characterization of novel natural fiber from *Saccharum bengalense* grass (Sarkanda). *Journal of Natural Fibers*, *17*(12), 1739–1747. https://doi.org/10.1080/15440478.2019.1598914

Wahid, M. K., Jumaidin, R., Mohd Suan, M. S., & Md Yusof, F. A. (2023). Characterisation of *Axonopus compressus* fibre through chemical composition, thermogravimetric behaviour, and moisture content evaluation. *Journal of Advanced Research in Fluid Mechanics and Thermal Sciences*, *110*(1), 172–181. https://doi.org/10.37934/arfmts.110.1.172181

Yuan, J., Liu, G., Liu, P., & Huang, R. (2024). Comprehensive assessment of elephant grass (*Pennisetum purpureum*) stalks at different growth stages as raw materials for nanocellulose production. *Tropical Plants*, *3*, e013. https://doi.org/10.48130/tp-0024-0013

Zaini, N., Tilova, A. M., Umami, N., Hanim, C., Astuti, A., & Suwignyo, B. (2021). Effect of harvesting age of chicory (*Cichorium intybus*) on the pattern of planting intercropping dwarf elephant grass in the second regrowth on production and quality. In *IOP Conference Series: Earth and Environmental Science* (Vol. 788, No. 1, p. 012173). IOP Publishing. https://doi.org/10.1088/1755-1315/788/1/012173

Zhang, B., Guo, Y., Liu, X., Chen, H., Yang, S., & Wang, Y. (2020). Mechanical properties of the fiber cell wall in *Bambusa pervariabilis* bamboo and analyses of their influencing factors. *BioResources*, *15*(3), 5316–5327. https://doi.org/10.15376/biores.15.3.5316-5327

Zhang, W., Zhang, S., Lu, X., Li, C., Liu, X., Dong, G., & Xia, T. (2020). Tissue-specific transcriptome analysis reveals lignocellulose synthesis regulation in elephant grass (*Pennisetum purpureum* Schum). *BMC Plant Biology*, *20*, 528. https://doi.org/10.1186/s12870-020-02735-3

Zor, M., Şen, F., Yazıcı, H., & Candan, Z. (2023). Thermal, mechanical and morphological properties of cellulose/lignin nanocomposites. *Forests*, *14*(9), 1715. https://doi.org/10.3390/f14091715